Pak. J. Bot., 48(5): 2031-2038, 2016.

STUDIES ON TWO ECONOMICALLY AND MEDICINALLY IMPORTANT PLANTS, *RHODIOLA CRENULATA* AND *RHODIOLA FASTIGIATA* OF TIBET AND SICHUAN PROVINCE, CHINA

TAO LI* AND XUAN HE

Department of Natural Medicine, Sichuan University, West China School of Pharmacy, No. 17, Section 3, Ren-Min-Nan-Lu Road, Chengdu, Sichuan 610041, P. R. China
**Corresponding author's email: scdxlitao@scu.edu.cn (T. LI)*

Abstract

Taxonomic assessment of two species of *Rhodiola*, *Rhodiola crenulata* and *Rhodiola fastigiata* was carried out and compared with two famous species, *Rhodiola rosea* and *Rhodiola pachyclados*. HPLC and Fourier Transform Near-Infrared (FT-NIR) spectroscopy techniques with the discriminant analysis and partial least squares regression (PLS) analysis were used for identification, classification, standardization and quality control of these species, *Rhodiola crenulata* and *Rhodiola fastigiata*. A rapid, nondestructive and innovative Fourier transform Near-Infrared spectroscopy analysis method with chemometrics techniques for qualitative and quantitative measurement of rhodionin was developed. On the basis of WHO recommendation utilizing authentic techniques as HPLC and Near-Infrared spectroscopy, it is ascertained that *Rhodiola crenulata* and *Rhodiola fastigiata* are two distinct species of Sichuan province and Tibet in China.

Key words: Fourier transform near-infrared spectroscopy; HPLC; *Rhodiola crenulata*; *Rhodiola fastigiata*; Rhodionin; Partial least squares; Discriminant analysis.

Introduction

Rhodiola species are largely distributed in the plateau areas in western Sichuan province and Tibet in China. In China, *Rhodiola* species have been used in traditional Tibetan medicines for over a millennium (Yang *et al.*, 1991). The only *Rhodiola* species, *R. crenulata*, which is recorded in the Pharmacopoeia of China (2015), has very significant economic and medicinal value. In recent years, many researches have been carried out on *Rhodiola* plants (e.g. many different pharmacological activities have been reported for anti-fatigue, anti-anoxia, antioxidant, anti-aging, and anti-tumor, etc.) (Xu *et al.*, 1998; Díaz Lanza *et al.*, 2001; Iaremiĭ & Grigor'eva, 2002; Kucinskaite *et al.*, 2004; Kanupriya *et al.*, 2005). Our study is on both aspects i.e. botanical and medicinal. Another species of *Rhodiola* i.e. *R. fastigiata* not only has the same efficacies as *R. crenulata*, but also has a wide distribution. Therefore, *R. fastigiata* has always been used an alternative to *R. crenulata* in Tibetan areas. Moreover the appearance of rhizome and root in *R. crenulata* is similar to *R. fastigiata*. Therefore, in order to differentiate and identify both the species correctly a near-infrared (NIR) spectroscopy model with the discriminant analysis method has been built to identify the two species more quickly and efficiently.

WHO, European, German and British herbal Pharmacopeias requirements are the authenticity of the plant material and that can be established based on taxonomy, chemotaxonomy, macroscopic and microscopic studies, botanical aspects (powder drug studies), chemical tests for quality control, qualitative and quantitative analysis by modern techniques such as HPLC, FT-IR, FT-NIR, etc. This work is also based on the same methods mentioned in WHO recommendation (Anon., 1997; Anon., 2000).

In this research article, we are presenting the differences among the species of *Rhodiola* because several species are available in local and international market with the same name and that affects the efficacy and economy of the country.

This research work was carried out with the aim to i) describe both plants from taxonomic point of view, ii) identification of plants based on chemical constituents (by qualitative & quantitative analysis) (Anon., 1997; Anon., 2000), iii) economic impact, from selling of plants in the world market.

Materials and Methods

Sample preparation During research 49 samples of rhizome and root of *R. crenulata* and 43 samples of *R. fastigiata* were collected from the plateau areas in western Sichuan province and Tibet in China from 2013 to 2015 for correct identification and chemical constituents' quantitative analysis. Botanical description is given in Table 1 and Fig. 1.

We identified the samples of the two species of *Rhodiola*, *R. crenulata* and *R. fastigiata*. In this regard all samples were continuously numbered, the localities (collection places) of *R. crenulata* and *R. fastigiata* are presented in Table 2(a) and 2(b). All of the samples of *Rhodiola*, *R. crenulata* and *R. fastigiata*, were pulverized into fine powder, and the powder samples were dried under a reduced pressure at 50°C for 12 h. All the voucher specimens of *Rhodiola*, *R. crenulata* and *R. fastigiata*, were preserved in the Herbarium (WCU) of Pharmacognosy of West China School of Pharmacy, Sichuan University. And the reference compound of rhodionin was prepared according to the method of Li & Zhang (2008). The analytical methods used in this research are given below.

NIR spectra collection: Near-infrared reflectance spectra were obtained by Thermo Antaris Ⅱ FT-NIRS analyzer (USA) equipped with an InGaAs detector. Spectral data collection, preliminary spectral data manipulation and instrument control, were performed using TQ Analyst software (version 8.0) (Li & He, 2016). 32 scans per spectrum were computed with 8 cm^{-1} resolution across the wavelength range of 4000-10000 cm^{-1} and ran in triplicate. The raw NIR spectra of *R. crenulata* and *R. fastigiata* samples are shown in Fig. 2(a) and 2(c).

Table 1. Morphological characteristic of *Rhodiola* species along with habit, habitat, phenology, reported chemical compounds, world market price and distribution.

Latin name	*R. crenulata*	*R. fastigiata*	*R. rosea*	*R. pachyclados*
Family	crassulaceae	crassulaceae	crassulaceae	crassulaceae
Habit	perennial dioecious herb	perennial dioecious herb	perennial dioecious herb	perennial monoecious herb
Root	main root robust, lateral root slender	main root cylindrical or long conical	erect, robust	fibrous
Rhizome	few branched, short, caudex leaves scalelike, oblanceolate	simple or few branched, caudex leaves scalelike, triangular	short, caudex leaves scalelike	slender, radical leaves forming rosette
Stem	numerous, erect or flabellate, straw-colored to red, 5-20 cm	4-10, arising from caudex apex, 8-20 cm	10–30 cm	1 in each rosette, simple, ascending-erect, 1-3 cm
Leave	shortly pseudopetiolate, elliptic-oblong to suborbicular, margin entire and undulate to crenate, apex obtuse to mucronate	linear-oblong, linear-lanceolate, elliptic, or oblanceolate, margin entire but finely mammillate, apex obtuse	sessile, oblong, elliptic-oblanceolate, or obovate, margin entire, apically few dentate, or serrate, apex acute to acuminate	sessile, entire, apex round, obovate, spathulate-obovate
Inflorescence	corymbiform, many flowered	corymbiform, dense	capitate, compact, many flowered	cyme-fascicles, 2-10 flowered
Flower	unisexual, large, male ones unequally 5-merous, sepals narrowly triangular, lanceolate, or oblong, petals red to purplish red, oblanceolate, stamens 10, nectar scales quadrangular, or oblong, carpels lanceolate to oblong	unisexual, male ones unequally 5-merous, sepals linear to narrowly triangular, petals red, oblong-lanceolate, stamens 10, nectar scales transversely oblong, apex emarginated, carpels erect, lanceolate	unisexual, male ones unequally 4-merous, sepals lanceolate-linear, petals greenish yellow or yellow, linear-oblanceolate to oblong, stamens 8, nectar scales oblong, carpels erect	bisexual, 5-merous, calyx oblong, petals oblong-spathulate, narrowly elliptic, entire, stamens 10, nectar scales oblong to broadly oblong, carpels 5
Fruit	follicles erect, red when dry	follicles erect, apex recurved	follicles lanceolate to linear-lanceolate	follicles 5
Seed	obovoid to ovoid, winged at both ends	–	lanceolate, winged at one end	ellipsoid
Habitat	thickets, grassland slopes, schist on mountain slopes, rocky places, rock crevices, 2800-5600 m	rocky slopes, 3500-5400 m	forested, grassy, or rocky slopes, 1800–2700 m	Kurram valley, 2000-3500m
Phenology	Fl. Jun-Sep.	Fl. Jun-Aug, fr. Sep.	Fl. Apr–Aug, fr. Jul–Sep.	–
Distribution	Qinghai, Sichuan, Xizang, Yunnan Bhutan, Nepal, Sikkim	Sichuan, Xizang, Yunnan Bhutan, India, Kashmir, Nepal, Sikkim	Gansu, Hebei, Jilin, Shanxi, Xinjiang Japan, Kazakstan, Korea, Mongolia, Russia, Europe, North America	Afghanistan, Pakistan
Reported chemical compounds	rhodionin, salidroside, *p*-tyrosol, rhodiosin, 6-O-galloylsalidroside, crenulatin, gallic acid, gallic acid ethyl ester, β-sitosterol, kaempferol, kaempferol 7-O-α-L-rhamnopyranoside, crenuloside, ellagic acid	rhodionin, rhodiolin, salidroside, *p*-tyrosol, daucosterol, dihydrokaempferol, β-sitosterol, gallic acid, gallic acid ethyl ester, daucosterol, herbacetin-8-arabinoside, 4'-methoxyl herbacetin	rosavin, rosin, rosarin, rosiridin, salidroside, *p*-tyrosol, rosiridol, rosiridine, gossypetin-7-O-L-rhamnopyranoside, rhodioflavonoside, daucosterol, lotaustralin, β-sitosterol, rhodioniside, rhodiolin, gallic acid, kaempferol	not reported
World market price	300g 40.00 $	–	300g 27.00 €	–

Table 2(a). Source of the 49 samples of *R. crenulata*.

Sample No.	Locality	Date of collection
1 - 5	Wenchuan, Sichuan	August, 2014
6 - 10	Xiaojin, Sichuan	July, 2014
11 - 15	Baoxing, Sichuan	July, 2014
16 - 20	Jiulong, Sichuan	September, 2013
21 - 25	Songpan, Sichuan	August, 2013
26 - 30	Heishui, Sichuan	July, 2013
31 - 35	Linzhi, Tibet	September, 2013
36 - 40	Hailuogou, Sichuan	July, 2014
41 - 45	Danba, Sichuan	August, 2014
46 - 48	Kangding, Sichuan	July, 2014
49	Hongyuan, Sichuan	August, 2013

Table 2(b). Source of the 43 samples of *R. fastigiata*.

Sample No.	Locality	Date of collection
1 - 5	Wenchuan, Sichuan	August, 2014
6 - 10	Xiaojin, Sichuan	July, 2014
11 - 15	Baoxing, Sichuan	July, 2015
16 - 20	Jiulong, Sichuan	September, 2013
21 - 25	Songpan, Sichuan	August, 2013
26 - 30	Heishui, Sichuan	July, 2013
31 - 35	Linzhi, Tibet	September, 2013
36 - 40	Hailuogou, Sichuan	July, 2014
41 - 43	Danba, Sichuan	August, 2014

Fig. 1. The plants, rhizome and root of *R. crenulata* (a, c) and *R. fastigiata* (b, d).

HPLC analysis: After spectral collection, HPLC which was regarded as the reference quantitative determination method was used to the analysis of rhodionin (Anon., 2000). And the concentration ranges for rhodionin in *R. crenulata* and *R. fastigiata* are presented in Fig. 3(a) and 3(b). The 0.3 g of powdered material sample was weighed in a stoppered Erlenmeyer flask for each sample, and extracted with 25 mL of methanol for 60 min by ultrasonic wave. Each stoppered Erlenmeyer flask's gross weight containing powdered material and 25 mL of methanol was weighed before and after methanol extraction treatment, filled lost weight with methanol. A portion of the extraction solution was centrifuged about 10 min, and filtered through a 0.45μm millipore membrane filter. Eventually, the injection volume was 10 μL and all samples were injected into the HPLC apparatus.

The concentrations of rhodionin in *R. crenulata* and *R. fastigiata* were determinated using Shimadzu LC-10AT HPLC apparatus (Japan). HPLC separation was performed on a Shim-pack VP ODS column (150 mm × 4.6 mm, 5 μm) using methanol-water (45:55, v/v) as mobile phase at a flow rate of 1.0 mL/min. The UV detection was performed at 332 nm, and the column temperature was 35ºC.

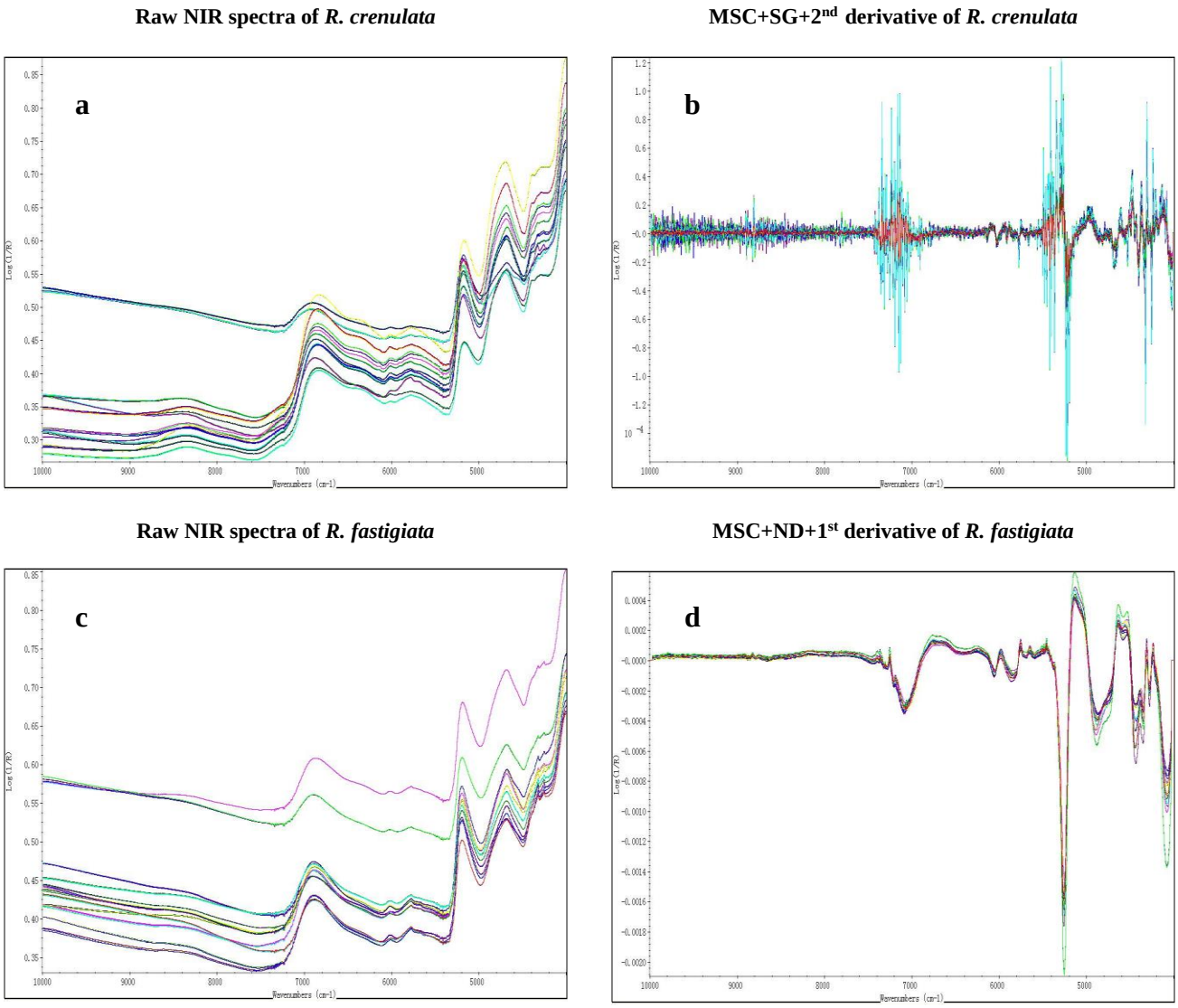

Fig. 2. Raw NIR spectra (a) and MSC+SG+2nd derivative (b) of *R. crenulata*; raw NIR spectra (c) and MSC+ND+1st derivative (d) of *R. fastigiata*.

NIR data preprocessing: While collecting the NIR spectral data, it is necessary to preprocess the NIR spectra data removing the scatter effect, noise and baseline drift when modeling by discriminant analysis and PLS. For the classification of *Rhodiola* species, discriminant analysis was applied. For the quantification of rhodionin, PLSR was adopted. In the TQ Analyst 8.0 software, data pre-treatment methods such as none (raw spectral data), first derivative analysis, second derivative analysis, standard normal variate (SNV) correction, smoothing, and multiplicative scatter correction (MSC) transformation were included.

As can be seen in Fig. 2(b) and 2(d), MSC method (Maleki *et al*., 2007) was used to remove the slope variation and to correct scatter effect, while, the SNV correction transformation was used to decrease the variation of the spectrum generated by varying particle size and scattering (Barnes *et al*., 1989). The frequently utilized smoothing methods were the Savitzky-Golay (SG) filter and Norris derivative (ND) filter (Zimmermann & Kohler, 2013). Moreover, the processing by first and second spectral derivative both was performed to enhance spectral resolution and remove baseline drift well (Rinnan *et al*., 2009).

Results and Discussions

The morphological characteristics of both species, *R. crenulata* and *R. fastigiata*, indicate that both are not similar (Table 1 and Fig. 1), but are sold with the same name (local name) in the local and international herbal market.

Both species *R. crenulata* and *R. fastigiata* have similar type of chemical compounds such as rhodionin. Another compound crenulatin is present only in *R. crenulata* (Table 1). FT-NIR and HPLC also support the existence of these compounds in both the species.

There are other two species of *Rhodiola*, *R. rosea* and *R. pachyclados* (Table 1), are available in the market and are sold with the same name but these are quite different from *R. crenulata* and *R. fastigiata*. *R. rosea* is sold in local market of USA, Europe, Russia, etc. and is very expensive because of therapeutic value (300 gram cost 27 € or near 40 $). The chemical constituents of *R. rosea* are quite similar to *R. crenulata* and having the same efficacy and pharmacological action.

In this research we used HPLC and FT-NIR as standardizing tool, as is recommended by WHO (Anon., 2000). As we have already mentioned in our aims, this research was carried out on two plants of medicinal and economic importance, *R. crenulata* and *R. fastigiata* and compared with *Rhodiola rosea*. *Rhodiola pachyclados* has also same properties as other three but till to date no chemical work has been published on this species. The morphologic characteristic comparison of species of *Rhodiola* along with habit, habitat, phenology, reported chemical compounds, world market price and distribution is presented in Table 1 (Fu & Ohba, 2001; Sarwar, 2002). The plants, rhizome and root of *R. fastigiata* and *R. crenulata* are illustrated in Fig. 1.

Delimitation of two *Rhodiola* species with discriminant analysis: Discriminant analysis was processed on the full-spectrum data to calibrate and verify the separation of the two different *Rhodiola* species. The obtained spectra were pretreated with the SNV mathematical transformation, ND filter, and 2nd derivative, which established the model for separation. In discriminant analysis method, Mahalanobis Distance was used to express the degree of separation of *R. crenulata* and *R. fastigiata*.

The results of discriminant analysis demonstrated that each species formed a well-defined cluster. There was a distinct boundary between *R. crenulata* and *R. fastigiata. R. fastigiata* cluster was formed on the left side of the graph, Whereas *R. crenulata* cluster appeared on the right side and there was no overlapping in models (Fig. 4). Therefore, the samples of two *Rhodiola* species were classified clearly. And the validation set of each model was selected and calculated for several times so that a good classification performance of qualitative analysis was obtained.

Selection of validation set in PLS models For NIR modeling with PLS algorithm, the samples in *R. crenulata* and *R. fastigiata* were both divided into two sets: the validation set and the calibration set for modeling analysis with the ratio of approximately 1:4. For each NIR model, models would be considered as robust and precise by the validation set and the calibration set for modeling analysis. There were 4 plans to select the optimal calibration and validation set, thereby reducing the bias in subset division. Based on the sample number of *R. crenulata* and *R. fastigiata*, the first 8 samples of *R. crenulata* were selected in the validation set (7 chosen samples of *R. fastigiata*) as plan A; the last 8 samples of *R. crenulata* were selected (7 chosen samples of *R. fastigiata*) as plan B; the 8 samples in the middle of *R. crenulata* were selected (7 chosen samples of *R. fastigiata*) as plan C; 1 of every 6 samples of *R. crenulata* were selected, and a total of 8 samples of *R. crenulata* and 7 samples of *R. fastigiata* were chosen as plan D finally.

Optimization models of NIR The correlation coefficient (R^2), root mean square error of prediction (RMSEP), and root mean square error of calibration (RMSEC) values in each NIR model of *R. crenulata* and *R. fastigiata* were obtained. Generally, a NIR calibration model with lower RMSEP and higher R^2 always perform well (Niu *et al.*, 2012).

According to Table 3(a), in plan D, the optimized rhodionin model of *R. crenulata* was developed with the spectral pretreatment methods: MSC mathematical transformation, second derivative analysis, and SG filter. Also, according to Table 3(b), in plan A, the optimized rhodionin model of *R. fastigiata* was developed with the spectral pretreatment methods: MSC mathematical transformation, first derivative analysis, and ND filter.

As shown in Table 4, the optimal NIR model of rhodionin for *R. crenulata* showed that the R^2, RMSEC, and RMSEP values were 0.98400, 0.0533, and 0.0347, respectively. The optimal NIR model of rhodionin for *R. fastigiata* showed that the R^2, RMSEC, and RMSEP values were 0.98424, 0.00455, and 0.00171, respectively. Therefore, the results indicated that the NIR models of *R. crenulata* and *R. fastigiata* both had good performance. Moreover, the R^2 in both Fig. 5a and 5b indicate a good correlation between NIR and HPLC values as to the content of rhodionin.

The optimization model's evaluation and validation: Fig. 3a and 3b clearly demonstrate that the concentration of rhodionin in *R. crenulata* and *R. fastigiata* measured by HPLC and NIR technique are very similar. In order to evaluate and validate the stability and veracity of NIR models of *R. crenulata* and *R. fastigiata* for rhodionin, the accuracy and precision were considered as the key parameters.

Precision: The intra-day and inter-day precision of rhodionin by NIR optimization models were verified, the intra-day precision was measured by analysing three concentrations of rhodionin three times within a day, and the inter-day variability was measured within four consecutive days.

As shown in Table 5, that the intra-day and inter-day precision assay both had well results with RSD less than 5.0% at each level of concentration for *R. crenulata* and *R. fastigiata* NIR model. Therefore, both the models demonstrated to have good precision.

Accuracy: This accuracy represented the level of veracity and similarity between the HPLC and NIR technique. In this part, not only recovery test, T and F tests, but also some factors values: RMSEP, RE and RSD were carried to evaluate the accuracy of the optimized NIR models.

The recovery rate at three known concentration levels represented for accuracy, too. Each optimization model determined six samples for three levels in the validation set, then the average recovery rate of each concentration level was calculated. As can be seen in Table 5, the results of recovery test of *R. crenulata* and *R. fastigiata* NIR models are between 95.5% and 106.5% while the RSD is less than 5.0% and RE is less than 5.5% for the objects.

The two optimal NIR models for *R. crenulata* and *R. fastigiata* were used to quantify the concentration of rhodionin in validation set' samples, respectively. As shown in Table 4, RMSEP in the NIR model of *R. crenulata* and *R. fastigiata* were 0.0347 and 0.00171, respectively. Moreover, the values of validation sets in optimized NIR models are listed in Table 6. Meanwhile, the results of T and F tests (with $p>0.05$) both indicated that HPLC method and NIR method showed no significant difference (Zhao *et al.*, 2007).

According to Tables 5 and 6, the results of evaluation and validation demonstrated that NIR optimization models of *R. crenulata* and *R. fastigiata* are repeatable, accurate, reliable, stable, and have good performance for quantitative determination of rhodionin in *R. crenulata* and *R. fastigiata*.

Table 3(a). PLS results for rhodionin in *R. crenulata* obtained using different spectra processing methods.

Preprocessing	Plan A			Plan B			Plan C			Plan D		
	R^2	RMSEC	RMSEP	R^2	RMSEC	RMSEP	R^2	RMSEC	RMSEP	R^2	RMSEC	RMSEP
MSC+SG	0.98349	0.0589	0.3230	0.99378	0.0348	0.1320	0.98487	0.0562	0.0911	0.98191	0.0567	0.0584
MSC+SG+1st derivative	0.98617	0.0539	0.2210	0.99501	0.0321	0.1230	0.98650	0.0531	0.1310	0.98376	0.0537	0.0467
MSC+SG+2nd derivative	0.95050	0.1010	0.0941	0.99510	0.0309	0.1110	0.98834	0.0494	0.1340	0.98400	0.0533	0.0347
MSC+ND+1st derivative	0.98405	0.0578	0.3280	0.99399	0.0342	0.1270	0.96997	0.0788	0.0554	0.96613	0.0772	0.0462
MSC+ND+2nd derivative	0.93832	0.1130	0.1370	0.99251	0.0381	0.1370	0.98623	0.0536	0.1120	0.98319	0.0546	0.0484
SNV+SG	0.96268	0.0881	0.1630	0.99406	0.0340	0.1290	0.98363	0.0584	0.1520	0.98196	0.0566	0.0578
SNV+SG+1st derivative	0.97286	0.0753	0.1570	0.99522	0.0305	0.1230	0.98676	0.0526	0.1310	0.98394	0.0534	0.0452
SNV+SG+2nd derivative	0.95250	0.0991	0.0805	0.99458	0.0325	0.1160	0.98892	0.0481	0.1450	0.98356	0.0540	0.0347
SNV+ND+1st derivative	0.96941	0.0799	0.2250	0.98592	0.0522	0.1650	0.95472	0.0964	0.0851	0.94491	0.0979	0.0625
SNV+ND+2nd derivative	0.98459	0.0569	0.1080	0.99255	0.0380	0.1420	0.98617	0.0537	0.1080	0.98285	0.0552	0.0458

Table 3(b). PLS results for rhodionin in *R. fastigiata* obtained using different spectra processing methods.

Preprocessing	Plan A			Plan B			Plan C			Plan D		
	R^2	RMSEC	RMSEP	R^2	RMSEC	RMSEP	R^2	RMSEC	RMSEP	R^2	RMSEC	RMSEP
MSC+SG	0.97302	0.00593	0.00329	0.92038	0.01130	0.01770	0.98358	0.00521	0.00996	0.79856	0.01450	0.02640
MSC+SG+1st derivative	0.96324	0.00691	0.00646	0.98349	0.00523	0.00757	0.98889	0.00433	0.01260	0.99003	0.00339	0.01100
MSC+SG+2nd derivative	0.98693	0.00414	0.00797	0.98839	0.00439	0.01010	0.98990	0.00413	0.01640	0.98870	0.00360	0.01440
MSC+ND+1st derivative	0.98424	0.00455	0.00171	0.95905	0.00818	0.02340	0.98444	0.00512	0.01100	0.99160	0.00311	0.00950
MSC+ND+2nd derivative	0.98165	0.00490	0.00180	0.98082	0.00563	0.00711	0.98870	0.00436	0.00765	0.98840	0.00365	0.00949
SNV+SG	0.97920	0.00522	0.00195	0.91210	0.01180	0.02060	0.98272	0.00539	0.00981	0.98394	0.00429	0.00974
SNV+SG+1st derivative	0.97063	0.00619	0.00656	0.97756	0.00690	0.00859	0.98907	0.00429	0.01240	0.98199	0.00454	0.01420
SNV+SG+2nd derivative	0.98799	0.00397	0.00901	0.87749	0.01390	0.01310	0.99024	0.00460	0.01650	0.98888	0.00357	0.01480
SNV+ND+1st derivative	0.98521	0.00441	0.00184	0.94610	0.00936	0.02610	0.97950	0.00586	0.01400	0.99200	0.00303	0.00937
SNV+ND+2nd derivative	0.98192	0.00487	0.00194	0.97880	0.00592	0.00797	0.98852	0.00440	0.00743	0.98859	0.00362	0.00934

Table 4. Parameters of optimal calibration models by PLS analysis.

Model	Spectral pretreatment method	R^2	RMSEC	RMSEP	Spectrum region for measurement (cm^{-1})
Rhodionin NIR model in *R. crenulata*	Plan D+MSC+SG+2nd derivative	0.98400	0.0533	0.0347	7622.57 - 6806.97 5514.05 - 5123.54 4479.62 - 4034.28
Rhodionin NIR model in *R. fastigiata*	Plan A+MSC+ND+1st derivative	0.98424	0.00455	0.00171	6744.77 - 7611.37 5858.61- 5056.10 4577.51 - 4169.73

Table 5. The precision and recovery test of rhodionin by NIR optimization models.

	Precision test		Recovery test		
	Intra-day RSD (%)	Inter-day RSD (%)	Recovery (%)	RSD (%)	RE (%)
Rhodionin NIR model in *R. crenulata*					
Low-concentration	1.8926	4.9700	101.9186	4.4537	1.9186
Mid-concentration	2.3002	2.7769	97.4521	2.5385	-2.5479
High-concentration	2.1968	4.7563	106.2958	3.1405	3.3962
Rhodionin NIR model in *R. fastigiata*					
Low-concentration	4.7033	4.8713	105.0606	4.7873	5.0606
Mid-concentration	3.1415	4.4045	95.9021	3.7730	-4.0979
High-concentration	0.8400	0.6858	100.2065	0.7629	0.2065

Table 6. Results of validation sets for estimation by NIR optimization models.

Sample No.	Actual values by HPLC (mg/ml)	Calculated values by NIR (mg/ml)	RSD (%)	RE (%)
Rhodionin NIR model in *R. crenulata*				
6	0.0943	0.0915	4.7484	-3.0223
12	0.1520	0.1590	2.6940	4.5724
18	1.0784	1.1238	2.6789	4.2053
24	0.2485	0.2369	2.1320	-4.6680
30	0.2401	0.2289	2.5350	-4.6647
36	0.4408	0.4440	4.6393	0.7316
42	0.0729	0.0751	0.1332	3.0178
48	0.0215	0.0219	3.9955	1.7054
Rhodionin NIR model in *R. fastigiata*				
1	0.00366	0.00364	11.3720	-0.6826
2	0.00211	0.00223	3.2436	3.1759
3	0.00205	0.00214	4.8713	4.4212
4	0.00868	0.00831	2.2287	-4.3057
5	0.01401	0.01355	3.1415	-3.2495
6	0.00465	0.00442	4.4045	-4.9462
7	0.09639	0.09659	0.8400	0.2061

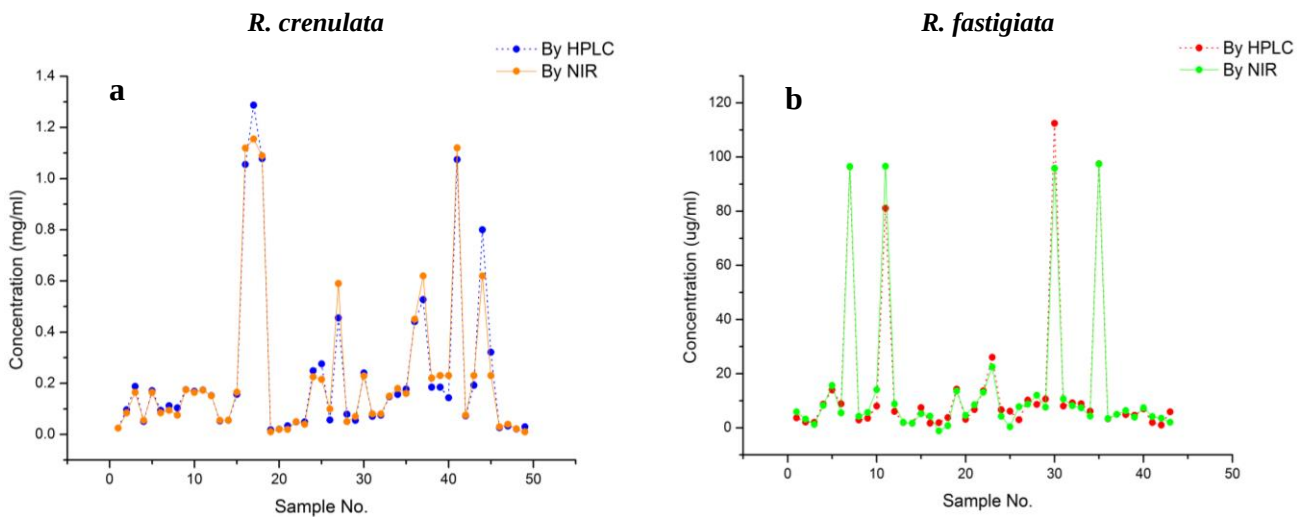

Fig. 3. The concentration of rhodionin in *R. crenulata* (a) and *R. fastigiata* (b) via HPLC method and NIR method.

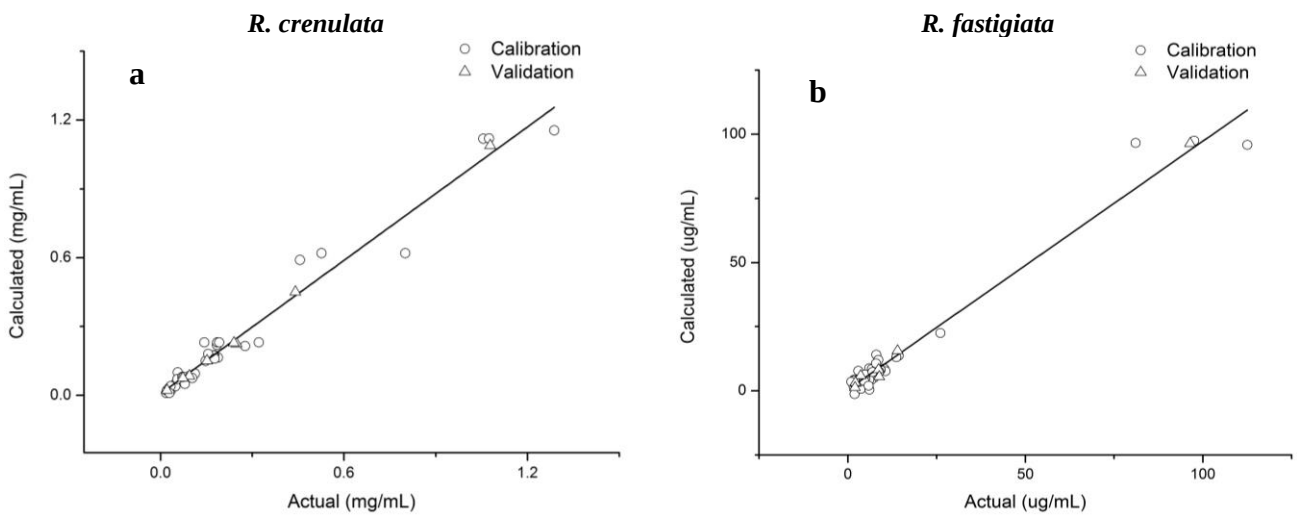

Fig. 5. Correlation diagrams of rhodionin in *R. crenulata* (a) and *R. fastigiata* (b) between the calculated values by NIR models and the actual values by HPLC.

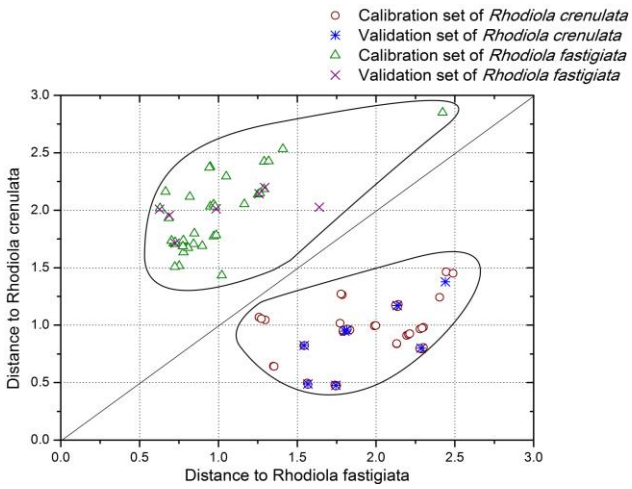

Fig. 4. Classification of *R. crenulata* and *R. fastigiata* by discriminant analysis method.

Conclusion

From our research it can be concluded that all four *Rhodiola* species, *R. crenulata*, *R. fastigiata*, *R. rosea*, and *R. pachyclados* are morphologically and chemically different, HPLC and NIR spectroscopy techniques with the discriminant analysis and PLS analysis provided a useful tool for quantitative as well as qualitative analysis. The discriminant analysis also supported the separation of *R. crenulata* and *R. fastigiata*, the NIR optimization models of PLS of *R. crenulata* and *R. fastigiata* provided a repeatable, accurate, stable, and precise quantitative determination of rhodionin in the two *Rhodiola* species which were important as traditional Tibetan medicinal plants and in traditional Chinese medicines. Compared with HPLC, the main and traditional method for quantitative analysis, NIR spectroscopy technique can be nondestructive. Moreover, the method is also fast and reliable. The results can offer technical supports for the further researches on rhodionin in *Rhodiola* plants. Also, this is a very promising, powerful technique which can be applied for the identification of *Rhodiola* species, classification, standardization and quality control.

Acknowledgments

This work was financed by Sichuan Science and Technology Department Applied Basic Research Project (2016JY0247) and Sichuan Education Department Research Fund (16ZA0006). We are also grateful to unknown referee for his great help and proofreading of the manuscript.

References

Anonymous. 1997. Guidelines for assessment of herbal medicine. WHO Expert Committee on specification for pharmaceutical preparations. Thirty fourth report. WHO. 1996 (WHO Technical Report, Series, No. 863) Annex 11. These guidelines are also included in quality assurance of pharmaceuticals: a compendium of guideline related materials, vol. 1. Geneva.

Anonymous. 2000. General Guidelines for methodologies on research and evaluation of traditional medicine. Geneva (WHO/EDM/TRM/2000.1)

Barnes, R.J., M.S. Dhanoa and S.J. Lister. 1989. Standard normal variate transformation and detrending of near-infrared diffuse reflectance spectra. *Appl. Spectrosc*, 43: 772-777.

Díaz Lanza, A.M., M.J. Abad Martínez, L. Fernández Matellano, C. Recuero Carretero, L. Villaescusa Castillo, A.M. Silván Sen and P. Bermejo Benito. 2001. Lignan and phenylpropanoid glycosides from *Phillyrea latifolia* and their in vitro anti-inflammatory activity. *Planta Med.*, 67: 219-223.

Fu, K.J. and H. Ohba. 2001. *Flora of China vol.8*. Science Press, Beijing. Missouri Botanical Garden Press, St. Louis.

Iaremiĭ, I.N. and N.F. Grigor'eva. 2002. Hepatoprotective properties of liquid extract of *Rhodiola rosea*. *Eksp. Klin. Farmakol*., 65: 57-59.

Kanupriya, D. Prasad, M. Sai Ram, R. Kumar, R.C. Sawhney, S.K. Sharma, G. Ilavazhagan, D. Kumar and P.K. Banerjee. 2005. Cytoprotective and antioxidant activity of *Rhodiola* imbricata against tert-butyl hydroperoxide induced oxidative injury in U-937 human macrophages. *Mol. Cell. Biochem.*, 275: 1-6.

Kucinskaite, A., V. Briedis and A. Savickas. 2004. Experimental analysis of therapeutic properties of *Rhodiola rosea* L. and its possible application in medicine. *Medicina* (*Kaunas*), 40: 614-619.

Li, T. and H. Zhang. 2008. Identification and comparative determination of rhodionin in traditional tibetan medicinal plants of fourteen *Rhodiola* species by high-performance liquid chromatography-photodiode array detection and electrospray ionization-mass spectrometry. *Chem. Pharm. Bull.*, 56: 807-814.

Li, T. and X. He. 2016. Quantitative analysis of salidroside and *p*-tyrosol in the traditional Tibetan medicine *Rhodiola crenulata* by fourier transform near-Infrared spectroscopy. *Chem. Pharm. Bull.*, 64: 289-296.

Maleki, M.R., A.M. Mouazen, H. Ramon and J. De Baerdemaeker. 2007. Multiplicative scatter correction during on-line measurement with near infrared spectroscopy. *Biosyst. Eng.*, 96: 427-433.

Niu, X.Y., Z.L. Zhao, K.J. Jia and X.T. Li. 2012. A feasibility study on quantitative analysis of glucose and fructose in lotus root powder by FT-NIR spectroscopy and chemometrics. *Food Chem.*, 133: 592-597.

Rinnan, A., F.V.D. Berg and S.B. Engelsen. 2009. Review of the most common preprocessing techniques for near-infrared spectra. *TrAC Trends Anal. Chem.*, 28: 1201-1222.

Sarwar, G.R. 2002. Crassulaceae In: *Flora of Pakistan* Vol. 209. (Eds.): S. I. Ali & M. Qaiser, Department of Botany, University of Karachi and Missouri Botanical Garden Press, USA. pp. 1-65.

Xu, J.F., P.Q. Ying and Z.G. Su. 1998. Study on application and development of resources of *Rhodiola* sachalinensis A. Bor. *Chinese Traditional and Herbal Drugs*, 29(3): 202-205.

Yang, Y.C., T.N. He, S.L. Lu, R.F. Hung and Z.X. Wang. 1991. *Zang Yao Zhi*. Qinghai People's Publishing House, Xining.

Zhao, X., H. Wang, J. You and Y. Suo. 2007. Determination of free fatty acids in bryophyte plants and soil by HPLC with fluorescence detection and identification by online MS. *Chromatographia*, 66: 197-206.

Zimmermann, B. and A. Kohler. 2013. Optimizing Savitzky-Golay parameters for improving spectral resolution and quantification in infrared spectroscopy. *Appl. Spectrosc.*, 67: 892-902.

(Received for publication 8 December 2015)